ELSEVIER

Geoderma 100 (2001) 321–353

GEODERMA

www.elsevier.nl/locate/geoderma

The chemistry of pedogenic thresholds

Oliver A. Chadwick [a,*], Jon Chorover [b]

[a] *Department of Geography, University of California, Santa Barbara, CA 93106, USA*
[b] *Soil Science Program, Department of Agronomy, Pennsylvania State University, University Park, PA 16802-3504, USA*

Received 10 January 2001; received in revised form 23 February 2001; accepted 1 March 2001

Abstract

Pedogenesis can be slow or fast depending on the internal chemical response to environmental forcing factors. When a shift in the external environment does not produce any pedogenic change even though one is expected, the soil is said to be in a state of pedogenic inertia. In contrast, soil properties sometimes change suddenly and irreversibly in a threshold response to external stimuli or internal change in soil processes. Significant progress has been made in understanding the thermodynamics and kinetics of soil-property change. Even in the open soil system, the direction of change can be determined from measures of disequilibrium. Favorable reactions may proceed in parallel, but the most prevalent and rapid ones have the greatest impact on product formation. Simultaneous acid–base, ion exchange, redox and mineral-transformation reactions interact to determine the direction and rate of change. The nature of the governing reactions is such that soils are well buffered to pH change in the alkaline and strongly acid regions but far less so in the neutral to slightly acid zones. Organic matter inputs may drive oxidation–reduction processes through a stepwise consumption of electron acceptors (thereby producing thresholds) but disequilibrium among redox couples and regeneration of redox buffer capacity may attenuate this response. Synthesis of secondary minerals, ranging from carbonates and smectites to kaolinite and oxides, forms a basis for many of the reported cases of pedogenic inertia and thresholds. Mineralogical change tends to occur in a serial, irreversible fashion that, under favorable environmental conditions, can lead to large accumulations of specific minerals whose crystallinity evolves over time. These accumulations and associated "ripening" processes can channel soil processes along existing pathways or they can force thresholds by causing changes in water flux and kinetic pathways.

Keywords: Pedogenesis; Inertia; Threshold

* Corresponding author. Tel.: +1-805-893-4223; fax: +1-805-893-8686.
E-mail addresses: oac@geog.ucsb.edu (O.A. Chadwick), jdc7@psu.edu (J. Chorover).

0016-7061/01/$ - see front matter
PII: S0016-7061(01)00027-1

1. Concepts of soil-property change

An underlying theme in pedology is related to the pattern of change in soil properties (cf. Bockheim, 1980; Johnson et al., 1990; McFadden and Knuepfer, 1990; Huggett, 1998; Birkeland, 1999). Why do specific properties change rapidly, slowly or not at all on some measurable time scale? Why do some soil features remain constant for periods of time and then change rapidly followed by another period of minimal change? Why do some soil properties become prominent (progressive evolution) only to diminish in importance later (regressive evolution)? Definitive answers to these questions form a Holy Grail for pedologists; over the past two to three decades our knowledge has grown greatly, but a comprehensive synthesis remains elusive. Here we review pertinent soil chemical theory and present field evidence collected along climosequences and chronosequences in the Hawaiian Islands to provide a basis for understanding the causes for rapid, irreversible change (thresholds) in soil properties.

Yaalon (1971) categorized soil properties into those that change rapidly, relatively slowly, and virtually not at all. Examples of properties that change quite rapidly (1 to 10^2 years) are those that respond to changes in external driving forces. Such properties include organic matter content, redistribution of salts, clays and sesquioxides, and formation or obliteration of mottles. Examples of properties that change slowly (10^2 to 10^3 years) are horizons of clay, iron-humus, or carbonate accumulation, whereas those that do not change for long periods of time (10^4 to 10^6 years) are characterized by large accumulations of secondary phases such as carbonates and opal, or profound depletions of soluble minerals leaving a nearly inert residue composed largely of iron oxides and kaolinite.

Persistence of soil properties in the face of changing external environmental factors led Bryan and Teakle (1949) to define "pedogenic inertia" as the case where a pedogenic process, once established, continues in spite of changes in the pedogenic environment to one that should not favor its continuation. Their concept was based on observations in Queensland, Australia that red, highly leached kaolinitic soils co-existed in landscapes with black, less-leached smectitic soils that formed later on sites where erosion had removed the original soil cover. The red soils formed under a wetter climate, but their properties persist even in the present drier climate because the pre-established chemical properties favor continued formation kaolinite clays. The term "pedogenic inertia" was an unfortunate choice because it assigns a physical term to a phenomenon that is mediated by physico-chemical processes.

In contrast, Muhs (1984) focused on pedogenic thresholds which he defined (following Schumm's (1979) definition for geomorphic thresholds) as "a limit of soil morphology stability that is exceeded either by intrinsic change in soil morphology, chemistry, or mineralogy or by a subtle but progressive change in

one of the external soil forming factors." In his paper, Muhs (1984) was particularly interested in intrinsic thresholds because they were less clearly identified in the literature than the case of extrinsic thresholds that are driven by external forcing factors (i.e., state factor analysis). Examples of intrinsic thresholds cited by Muhs (not meaning to be inclusive) were: (1) the need to leach excess Ca and Mg (powerful flocculators) from profiles prior to initiation of clay illuviation, (2) enhanced clay illuviation because of accumulation of exchangeable Na (powerful deflocculator) in excess of Ca and Mg, (3) calcium plugging of pores during the transition from calcic to petrocalcic horizon leading to lateral water movement and upward growth of laminar carbonate layers, (4) requirement for a minimum level of Fe and Al accumulation prior to sequestration of organic matter in Bhs horizons, (5) decrease in oxidized forms of crystalline pedogenic Fe due to a decrease in water movement efficiency caused by accumulation of pedogenic clays, and (6) change from a predominance of clay illuviation to vertic involution processes in soil profiles with increased concentration of smectite clays.

Other examples can be added to this list of thresholds: (1) rapid accumulation of clay in soil profiles once overall particle size is decreased by eolian accession (McFadden and Weldon, 1987; McFadden, 1988; Harden et al., 1991; McDonald et al., 1996); (2) increased erosion driven by formation of petrocalcic horizons leading to less efficient downward percolation of water (Wells et al., 1987), (3) increase in rainwater percolation depth due to pore plugging by carbonates and subsequent movement of water along occasional large cracks in duripans and petrocalcic horizons (Torrent and Nettleton, 1978; Gile and Grossman, 1979), (4) formation of vegetation-free sodic slickspots at the expense of nearby grassland soil because of degraded structure and poor infiltration caused by increased sodium levels and lower infiltration (Reid et al., 1993), (5) a shift from weathering derived to rainwater derived Sr and Ca due to rapid weathering of pumice with high surface area (Kennedy et al., 1998; Chadwick et al., 1999; Vitousek et al., 1999), and (6) a rapid shift toward greater acidity, wetness, and reduction in response to invasion of *Sphagnum* (Ugolini and Mann, 1979; van Breemen, 1995).

Accumulation of soil properties and their subsequent susceptibility to change is controlled to a great extent by self-enhancing feedback processes that increase a particular property until exhaustion of one or more of the reactants brings about a termination (Torrent and Nettleton, 1978). The acceleration of soil property accumulation driven by self-enhancing feedback processes is a major cause of the threshold examples cited above (cf. Reid et al., 1993; van Breemen, 1995). Similarly, a shift to self-terminating feedback processes can slow soil-property change, because if reactants are in short supply, a corresponding reaction is precluded even if the external driving factors would otherwise favor it. The thermodynamic properties of acid–base, oxidation–reduction and mineral synthesis reactions combine with kinetic factors such as water flux and tempera-

ture to control the nature of feedback processes. Here we summarize the behavior of the relevant chemical reactions in soils and their contribution to changing soil properties. Interestingly, parallel with soil chemical theory, intensive field studies demonstrate that threshold behavior in soil systems is much more common than has been appreciated previously.

2. Threshold reactions in pedogenesis

Chemical reactions in soils and the probability that they will occur are determined by the thermodynamics of the soil system. Soils are open systems; pedogenic transformations are driven by a continuous flux of matter and energy acting on a progressively modified parent material (Fig. 1). Solar radiation is a primary source of energy, and through photosynthesis it provides inputs of acidity and reducing power derived to a large extent from reduced carbon compounds. Other sources of acidity come from external sources such as volcanic gases and industrial pollutants. The energy state of the soil system is reduced when primary minerals, which are in disequilibrium with earth surface conditions, are transformed to more stable secondary phases. The consumption of protons and electrons during chemical reactions with parent material affects the trajectory of pedogenesis by determining pathways for mineral weathering and neosynthesis.

2.1. Acid–base reactions

A primary suite of chemical reactions in soil involves the production of acids by biodecay and their consumption through weathering of minerals in parent material or added as mineral aerosol. Soil development can be characterized as a long-term acid–base reaction in which acids from the atmosphere (CO_2, NO_2, SO_2) and those generated by the biota react with bases in the form of rock minerals to form secondary minerals and soil solution alkalinity (Fig. 1). These chemical reactions are superimposed on physical weathering processes that contribute to the availability of reactive surfaces and hydrologic flow paths. Water flux is a primary determinant of the rate and trajectory of soil development, since it carries reactants into the profile and contributes to down-gradient transport of solute and colloidal products. If the products of the acid–base reactions are carried out of soil profiles by infiltrating water, the soil system is acidified (i.e., its acid neutralizing capacity is decreased) and the water is alkalinized (i.e., its acid neutralizing capacity is enhanced) (van Breemen et al., 1983, 1984). In arid and semiarid regions, reaction products are deposited lower in the profile rather than being flushed from the soil, leading to spatially discretized alkalinization of the profile itself.

Under humid conditions, a progressive loss of soil acid neutralizing capacity (ANC(s), where s refers to the soil solid phase) accompanies the removal of

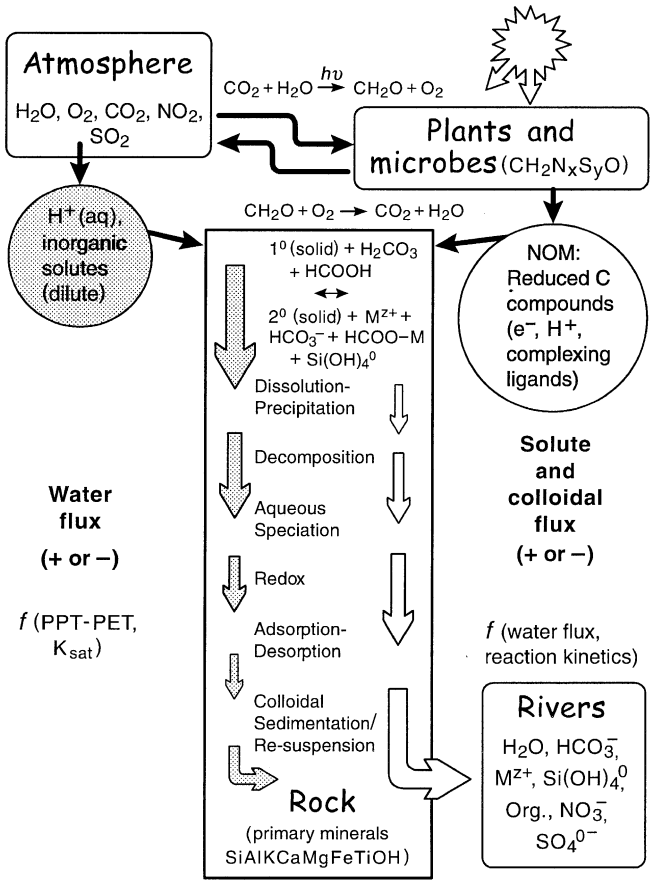

Fig. 1. Soil profiles are active mixing zones of living and dead organic matter, water, a trace gas laden atmosphere, decaying rock minerals and the residue of their interaction. The chemistry of pedogenesis is driven by solar energy both directly and through photosynthesis and gravitational energy through the movement of water through soil profiles. Water acts to mediate chemical reactions and to transport reactants and products through the profile. Mineral weathering acts as a sink for atmospherically and biospherically derived acids; the reaction products can accumulate within the profile or be lost through leaching. Reduced carbon compounds also provide ligands for complexing, reducing and leaching otherwise sparingly mobile cations. Chemical reaction rates are controlled both by the intensity of the extrinsic climatic factors and the intrinsic thermodynamic and kinetic properties of the soil system.

reaction products from the profile. The ANC(s) can be estimated by the component composition of the soil solid phase as determined by total elemental analysis (van Breemen et al., 1983):

$$\mathrm{ANC(s)} = 6[\mathrm{Al_2O_3}] + 2[\mathrm{CaO}] + 2[\mathrm{MgO}] + 2[\mathrm{K_2O}] + 2[\mathrm{Na_2O}] + 2[\mathrm{MnO}] + 2[\mathrm{FeO}] - 2[\mathrm{SO_3}] - 2[\mathrm{P_2O_5}] - [\mathrm{HCl}] \quad (1)$$

where brackets denote molar concentrations (mol m^{-3} soil) and stoichiometric coefficients denote the moles of protons consumed (positive values) or produced (negative values) during dissolution of the solid oxides. Fig. 2 sketches a hypothetical soil titration curve showing the progressive change in soil pH in response to addition of acid and the concomitant lowering of ANC(s). This figure, which depicts the sequence of chemical processes that buffer soil pH with decreasing ANC(s), can be viewed as the time-dependent acidification of an initially alkaline parent material.

During the early stages of acid addition there is little change in the alkaline pH because the soil contains carbonates of Ca, Mg and Na that neutralize the added acidity. Soil pH is buffered in the alkaline range when carbonate solids are present because of proton consumption and alkalinity generation that accompanies carbonate dissolution. This process can be generalized as:

$$M_{1-0.5x}Na_xCO_3(s) + H^+(aq) \leftrightarrow (1-0.5x)M^{2+}(aq) + xNa^+(aq) + HCO_3^-(aq) \quad (2)$$

where M represents Ca^{2+} and/or Mg^{2+}, and $0 \le x \le 2$. Eq. (2) shows a negative correlation between pH and the activities of Na^+, Mg^{2+}, Ca^{2+} and HCO_3^- in equilibrium with their respective carbonate solids. For calcite, the most prevalent pedogenic carbonate, M = Ca, $x = 0$ and log $K = 1.91$ for Eq. (2). In this case, Eq. (2) shows that soil solution pH decreases from pH 10 to 8

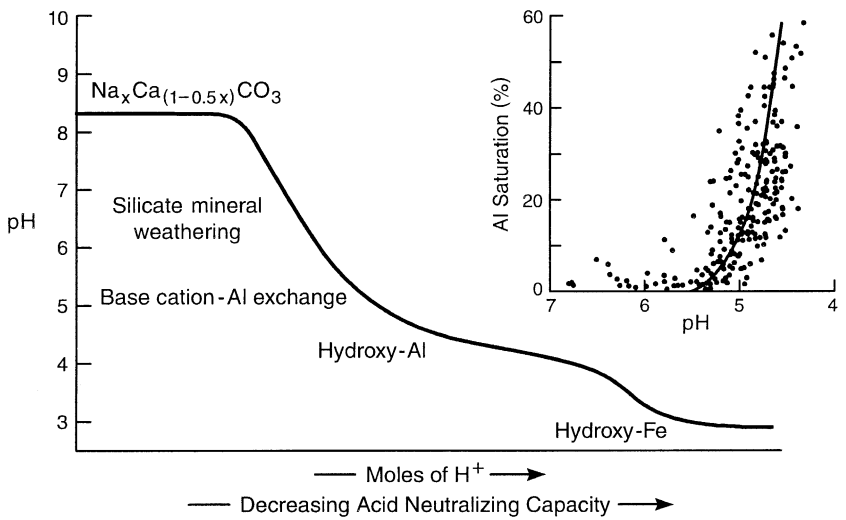

Fig. 2. Schematic titration curve showing the loss of soil acid neutralizing capacity with increasing addition of protons and its differential effect on pH depending on the type of chemical buffering reaction (modified from van Breemen et al., 1983). Inset shows the change in pH with increasing Al saturation (fraction of KCl extractable Al relative to CEC) of the exchange complex (modified from Thomas and Hargrove, 1984).

as the activities of Ca^{2+} and HCO_3^- [set equal to each other] increase from 10^{-4} to 10^{-3}. As long as Ma_2CO_3 and $CaCO_3$ are dominant soil components consuming acidity, the soil pH will be buffered in the alkaline pH range (Fig. 2). Once the carbonates are exhausted, there is a relatively rapid decline in pH during the weathering of primary minerals and as H^+ and Al^{3+} ions replace the non-hydrolyzing, so-called "base cations" (Ca^{2+}, Mg^{2+}, K^+, Na^+), on the exchange complex. The weathering reactions may be congruent or incongruent, depending largely on the aqueous speciation of soil solution.

For example, the incongruent dissolution of plagioclase, a Na–Ca–feldspar, to form smectite or kaolinite is promoted by proton attack when elevated CO_2 concentrations result from root respiration and organic matter decay:

$$2\underset{\text{(plagioclase)}}{Na_{0.5}Ca_{0.25}AlSi_3O_8}(s) + 0.5Mg^{2+}(aq) + 1.5CO_2(g) + 6H_2O(1) \leftrightarrow \underset{\text{(smectite)}}{Ca_{0.25}[Si_4]Al_{1.5}Mg_{0.5}O_{10}(OH)_2}(s) + Na^+(aq) + 0.25Ca^{2+}(aq) + 1.5HCO_3^-(aq) + 2Si(OH)_4^0(aq) + 0.5AlOH^{2+}(aq) \quad (3a)$$

$$2\underset{\text{(plagioclase)}}{Na_{0.5}Ca_{0.25}AlSi_3O_8}(s) + 2CO_2(g) + 11H_2O(1) \leftrightarrow \underset{\text{(kaolinite)}}{[Si_2]Al_2O_5(OH)_4}(s) + Na^+(aq) + 0.5Ca^{2+}(aq) + 2HCO_3^-(aq) + 4Si(OH)_4^0(aq) \quad (3b)$$

Reaction (3a) is favored where leaching conditions are not too intense such that cations and Si are available to form smectite, whereas reaction (3b) is favored under high leaching conditions where the soluble weathering products are removed extensively (see Section 3.3 below). For example, note the higher consumption of water and increased removal of silicic acid and calcium in Eq. (3b).

An alternative weathering pathway prevails when biogenic organic acids (e.g., oxalate, citrate) sequester reaction products (e.g., Al, Fe) into soluble complexes, thereby preventing the formation of secondary minerals. The congruent dissolution of plagioclase, for example, may be promoted by the prevalence of complexing ligands (e.g., oxalate):

$$2\underset{\text{(plagioclase)}}{Na_{0.5}Ca_{0.25}AlSi_3O_8}(s) + 2\underset{\text{(oxalate)}}{C_2O_4H_2}(aq) + 12H_2O(l) + 4CO_2(g) \leftrightarrow Na^+(aq) + 0.5Ca^{2+}(aq) + \underset{\text{(Al-oxalate complex)}}{C_2O_4Al^+}(aq) + 4HCO_3^-(aq) + 6Si(OH)_4^0(aq) \quad (4)$$

As a consequence of reactions (3a,b) and (4), cations are leached from the profile with charge balancing anions (e.g., HCO_3^- and organic acids), a process

that progressively lowers the ANC(s) and pH from near neutral to ca. pH 5.5 (Fig. 2). Comparison of these reactions illustrates the important role of water flux and acid production by biological activity (generation of CO_2 and organic acids) in accelerating mineral transformation reactions. In addition, soil solution chemistry, and aqueous speciation in particular, is a governing factor in weathering trajectories. For example, biogenic oxalate precludes secondary mineral formation by forming soluble complexes with Al and removing it from the locus of weathering. Metal–ligand complexes are mobile in percolating soil solution, and their translocation and deposition can lead to podzolization (Ugolini and Dahlgren, 1987). Even if removal is incomplete, the presence of complexing ligands, such as oxalate, permits the total equilibrium concentration of dissolved Al to exceed levels that could be achieved in their absence (Lindsay and Walthall, 1996).

Aqueous speciation is a critical determinant of all heterogeneous reactions in pedogenesis, including adsorption/desorption and precipitation/dissolution. Indeed, incipient horizonation of the soil profile may be revealed through analysis and speciation of soil solution even before a distinct effect is manifest at the field scale (Ugolini et al., 1988). The sharp changes (or thresholds) in soil solution chemistry that occur over small vertical distances in soil profiles reflect transitions between heterogeneous reactions. For example, ligand-promoted dissolution (Eq. (4)) in surface soils can give way to dominantly carbonation reactions (Eqs. (3a,b)) at depth, where soluble organic matter concentrations are smaller (Ugolini and Sletten, 1991). As shown in Eqs. (3a,b) and (4), the transition from organic to inorganic proton donors and complexing ligands can bear heavily on the nature of reaction products.

Mineral weathering is closely linked to the composition of the ion exchange complex because dissolved cations compete for cation exchange sites on existing and neo-formed soil clays. Proton adsorption to soil solids is often followed by rapid dissolution and readsorption of Al (Ritchie, 1995; Chorover and Sposito, 1995a). Selective readsorption of Al relative to Si is a primary cause for non-stoichiometric dissolution of aluminosilicates (Brady and Walther, 1989). The Al^{3+} cation is highly competitive with nutrient cations for exchange sites. For example, the binary exchange of Al^{3+} for Ca^{2+} on soil cation exchange sites (where X represents one mole of exchanger negative charge) is given by:

$$3CaX_2(s) + 2Al^{3+}(aq) \leftrightarrow 2AlX_3(s) + 3Ca^{2+}(aq) \quad (5)$$

Typical values for the conditional cation exchange coefficient ($^cK_{ex}$) for this reaction are in the range of 2.5–3.5 (Jardine and Zelazny, 1996). Furthermore, this reaction is more favorable at low ionic strength (i.e., increased throughput of freshwater) because of the difference in activity coefficients between trivalent Al and bivalent Ca (Reuss and Johnson, 1986; Reuss et al., 1990). Thus, for an acid soil solution containing 2×10^{-6} M Al^{3+} and 2×10^{-5} Ca^{2+}, at a total solution ionic strength of 2×10^{-4} M, Eq. (5) with $^cK_{ex} = 3$ predicts that 90%

of the cation exchange sites will be occupied by Al, despite a 10-fold higher concentration of Ca^{2+} in soil solution. This enhancement of exchangeable acidity is especially important below pH 5, when monomeric inorganic Al is dominantly in the form of Al^{3+} (see Eqs. (6a,b) below). Indeed, Thomas and Hargrove (1984) showed that the ratio of exchangeable acidity to total CEC increases dramatically from near zero at pH 5.5 to ca. 0.6 (i.e., Al saturation of 60%) at pH 4.5 for a large set of acidic US soils (Fig. 2—inset). This pH range, therefore, represents a threshold transition from an exchange complex dominated by non-hydrolyzing cations to one dominated by Al^{3+}, hydroxyl Al species and H^+. Since Al is more prevalent than base cations in crystal materials (Sparks, 1995), complete conversion from base cation to Al-saturated exchange sites can occur within a relatively narrow time-climate window of soil weathering (Section 3.3, see also Scott, 1963; Marshall, 1977; Chadwick et al., 1995; Vitousek et al., 1997; Kelly et al. 1998).

Weathering of primary minerals and leaching of base cations and silica, coupled with progressive conversion of soil exchange sites to dominance by Al, ultimately enriches the solid phase (both inorganic and organic) in surface polymeric species and hydroxides of Al (particularly gibbsite) (Jackson and Sherman, 1953; Jackson, 1965). As a result, Al plays a progressively greater role in buffering soil solution acidity. Gibbsite solubility increases with decreasing pH below neutrality and, once released from the solid phase, soluble Al is subjected to progressive hydrolysis. Both precipitation/dissolution of gibbsite (Eq. (6a)) and the hydrolysis of dissolved Al (Eqs. (6b and c)) are capable of consuming or producing significant amounts of soil solution acidity (Lindsay and Walthall, 1996; Nordstrom and May, 1996):

$$\underset{\text{(gibbsite)}}{Al(OH)_3(s)} + 3H^+(aq) \leftrightarrow Al^{3+}(aq) + 3H_2O(l) \qquad pK = -8.11 \text{ to } -10.8 \tag{6a}$$

$$Al^{3+}(aq) + H_2O(l) \leftrightarrow AlOH^{2+}(aq) + H^+(aq) \qquad pK = 4.99 \tag{6b}$$

$$AlOH^{2+}(aq) + H_2O(l) \leftrightarrow Al(OH)_2^+(aq) + H^+(aq) \qquad pK = 5.11 \tag{6c}$$

where the range in pK values for Eq. (6a) exemplifies the inverse dependence of mineral solubility on phase crystallinity (Sposito, 1994, see also Section 3.2). The total concentration of Al in acid soils is often assumed to be governed by gibbsite solubility as shown in Eq. (6a), (Reuss and Johnson, 1986; Robarge and Johnson, 1992), although it is also clear that solid-phase Al–organic complexes are an important source of dissolved Al in soils subjected to acidification (Cronan et al., 1986; Dahlgren and Walker, 1993; Mulder and Stein, 1994; Ritchie, 1995; Vance et al., 1996). In this case, a complexation equilibrium governs Al solubility:

$$AlX_3(s) + 3H^+(aq) \leftrightarrow Al^{3+} + 3HX(s) \tag{7}$$

This reaction follows from Eq. (5) and, in contrast to Eq. (6a), shows a dependence of Al dissolution on both pH and the composition of adsorption sites. If soil organic matter controls Al solubility, then progressive acidification, coupled with depletion of the organically bound Al pool, will diminish equilibrium Al concentrations at a given pH (Cronan et al., 1986; Mulder and Stein, 1994). In any case, the predominance of Al in most soils implies that it will buffer pH against a large amount of acid input and it is not quickly exhausted. In fact, most soils of humid environments are buffered by these reactions with Al.

Finally, in this example of progressive acidification (Fig. 2), solubility and hydrolysis of Fe can serve as a proton sink at pH < 4:

$$\underset{\text{(goethite)}}{\alpha - \text{FeOOH(s)}} + 3\text{H}^+(\text{aq}) \leftrightarrow \text{Fe}^{3+}(\text{aq}) + 2\text{H}_2\text{O(l)} \qquad \text{p}K = 0.9 \qquad (8a)$$

$$\text{Fe}^{3+}(\text{aq}) + \text{H}_2\text{O(l)} \leftrightarrow \text{FeOH}^{2+}(\text{aq}) + \text{H}^+(\text{aq}) \qquad \text{p}K = 2.2 \qquad (8b)$$

$$\text{FeOH}^{2+}(\text{aq}) + \text{H}_2\text{O(l)} \leftrightarrow \text{Fe(OH)}_2^+(\text{aq}) + \text{H}^+(\text{aq}) \qquad \text{p}K = 3.5 \qquad (8c)$$

These reactions would buffer the soil pH near 3. However, Fe(III) (oxy)hydroxide solids are much less soluble than their Al-bearing analogs. Because Al is so prevalent in soil, Fe is seldom solubilized due to low pH conditions. However, in contrast to Al, Fe may be removed from soil through reductive dissolution processes, as discussed in Section 3.3.

The exact characteristic of the pH/ANC(s) curve shown schematically in Fig. 2 will differ for each soil depending on the amount of reactants (Eq. (1)) and the kinetics of their removal. Soils of arid regions where reaction products are not removed will remain alkaline indefinitely, as governed by reactions (2) and (3a). In humid climates, the rate ANC(s) consumption decreases with time, as the kinetically labile solids are progressively depleted from the profile. Fig. 3 shows the decreasing rate of proton neutralization that accompanies soil development in Hawaiian basalts for a forested chronosequence subjected to 2500 mm of annual rainfall and a mean annual temperature of 16°C. The rate plotted on the *y*-axis was calculated from Eq. (1) and the proton stoichiometry included therein, using depth-weighted-mean total elemental analyses of the soils. High initial rates reflect the removal of rapidly dissolving phases such as volcanic glasses, olivines and amphiboles. Much lower rates in the older sites are consistent with the fact that only slowly dissolving minerals remain, dominantly kaolin and crystalline oxides of Al and Fe (Vitousek et al., 1997; Chorover et al., 1999).

The acid–base buffering reactions suggest predictions of where we expect to find pedogenic thresholds based on a consideration of acid input to soil. The rapid drop in pH with acid input from neutral to pH 5.5 compared with the considerable lag between acid input and a pH response in the alkaline (pH 7–9) and strongly acid (pH < 4.5) ranges suggests that globally there should be more soils with alkaline and strongly acid pH values than those that are neutral to

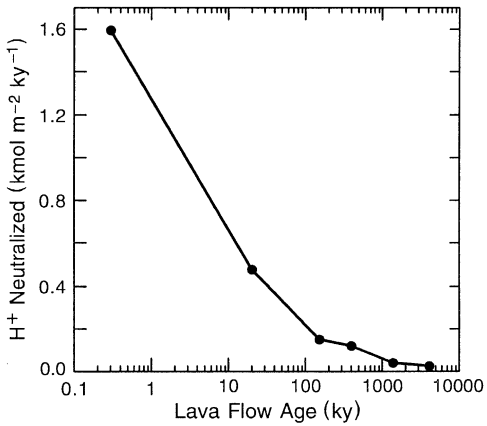

Fig. 3. The change in ANCs and hence the amount of H^+ neutralized along a chronosequence of soils sampled at 2500 mm average annual rainfall and 16°C in the Hawaiian Islands (Vitousek et al., 1997; Chadwick et al., 1999; Hotchkiss et al., 2000). The values for H^+ neutralized were calculated using Eq. (1), after taking into account soil collapse (see Vitousek et al., 1997).

slightly acid, and that the latter soils are unstable and can be expected to undergo rapid change under either arid or humid conditions.

2.2. Mineral stability

Chemical weathering of rock occurs because of the thermodynamic instability of primary minerals subjected to Earth surface conditions. When a parent material comprising a known suite of primary minerals is weathered in an aqueous environment, the composition of solid and solution phase reaction products at equilibrium can be predicted on the basis of chemical thermodynamics. The physicochemical properties of secondary minerals, especially aluminosilicate clays, play an enormous role in determining soil behavior because of their charge, high surface area, water and solute sorption and their colloidal properties (e.g. tendency to shrink and swell, aggregate and disperse). The same environmental conditions that determine pH are largely responsible for determining the nature and amount of secondary minerals in soil profiles.

The tendency for a mineral dissolution or formation reaction to occur under a set of chosen conditions is dictated by the Gibbs energy of reaction (ΔG_r):

$$\Delta G_r = RT \ln Q/K_{diss} \qquad [\mathrm{kJ\,mol^{-1}}] \tag{9}$$

where R is the universal gas constant [8.314×10^{-3} kJ mol^{-1} K^{-1}], T is temperature [K], K_{diss} is the equilibrium constant for the dissolution reaction (equivalent to the value of Q at equilibrium), and Q is the reaction quotient of product and reactant activities, raised to the power of their respective stoichiometric coefficients in the weathering reaction. A reaction proceeds ($\Delta G_r < 0$)

only if $Q/K_{diss} < 1$. For a congruent mineral dissolution reaction (no solid products formed), the value of Q/K_{diss} is known as the saturation index (Ω), because it provides a measure of solution phase saturation with respect to the solid phase (Stumm and Morgan, 1996). For a given soil solution composition, values of Ω may be calculated for all potential solids in order to assess the tendency for their precipitation or dissolution. The solids that control the equilibrium solubility of major elements (e.g., Al, Fe or Si) under specific pedogenic conditions may, therefore, be predicted (Lindsay, 1979). For example, congruent weathering reactions for Mg-smectite, allophane, kaolinite and gibbsite were used to construct the solubility diagrams in Fig. 4, with solid phases assigned unit activity. These plots show the effects of soil solution silicic acid ($Si(OH)_4^0$) and Mg^{2+} concentration on the identity of solid phases controlling Al solubility at three different pH values. At a constant silicic acid concentration, the most stable solid phase is that which supports the lowest aqueous Al concentration (Sposito, 1994). Evaluation of mineral stability fields in relation to environmental factors, and seasonal and inter-annual variation in soil solution composition provides a powerful tool for understanding present chemical processes and evaluating past chemical (and environmental) conditions.

Pedogenic thresholds can be traced to the type and amount of pedogenic products accumulated in soil profiles. For instance, the accumulation of kaolin minerals, gibbsite and crystalline iron oxides, which has been considered a case of pedogenic inertia (Bryan and Teakle, 1949), is more precisely an accumulation of solid phases that are stable thermodynamically at earth surface conditions (Jackson and Sherman, 1953; Jackson, 1965; Buol and Eswaran, 2000). In the case described by Bryan and Teakle (1949), prior depletion of Si precludes the

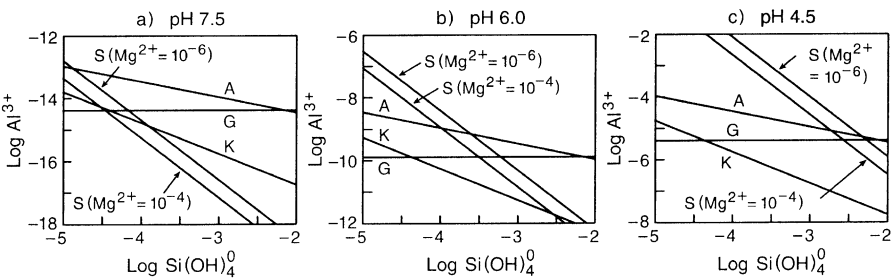

Fig. 4. Activities of dissolved Al^{3+} and $Si(OH)_4^0$ in equilibrium with secondary aluminosilicate minerals Mg-smectite (S), kaolinite (K), proto-imogolite allophane (A), and gibbsite (Al hydroxide) (G) as a function of decreasing pH: (a) pH 7.5, (b) pH 6.0, and (c) pH 4.5. Two lines for smectite show the effects of dissolved Mg^{2+}, which is the exchangeable cation and a constituent of the octahedral sheet in the smectite. At any fixed activity of silicic acid, the solid phase supporting the lowest equilibrium activity of Al^{3+} is favored in the long term. However, supersaturated solids supporting higher Al^{3+} activities may precipitate first if the kinetics of their formation are more rapid.

transformation of a kaolinitic soil into one dominated by smectite. The solubility diagrams shown in Fig. 4 indicate that this pedogenic "inertia" could be overcome only by sufficient increases in soil solution silicic acid—an unlikely event once primary silicates have been exhausted—or solution pH. Even though the present environmental conditions favor smectite formation from parent rock, the soil precursors are not available in the proper concentrations and combinations. At the other extreme, synthesis of smectite clays in a favorable (e.g., Fig. 4a) wetting and drying environment leads to clay translocation and genesis of an Alfisol. In time, enough clay is formed that water sorption leads to excessive swelling, churning of the soil mass and disruption of the horizon structure. The result is a threshold wherein the Alfisol is rapidly transformed into a Vertisol (Muhs, 1982). In this case, however, a long-term change to high leaching conditions might lower Si and base cation levels enough to favor kaolinite or gibbsite (Fig. 4). Slow weathering of the smectite would lead to a loss of shrink–swell capability.

Mineral transformation thresholds during pedogenesis can be exemplified using additional data from the Hawaiian chronosequence that was introduced in Fig. 3 (Hendricks et al., 1995; DiChiaro, 1998; Chorover et al., 1999). Fig. 5 shows that mineral transformation of basaltic ash and lava results in formation of short-range-ordered secondary minerals (e.g., allophane) and accumulation of 2:1 layer type silicates during the first 400 ka of soil development (Fig. 5a). During this time, solution pH and Si concentrations are sufficiently high to favor these "metastable" reaction products (Fig. 5b). However, after 400 ka, continued depletion of dissolved Si and further increases in H^+ concentration under high rainfall (Fig. 5b) force the weathering of allophane and 2:1 clays to kaolin (halloysite and kaolinite) and gibbsite (Fig. 5a). It is noteworthy that solution Al concentrations also decline during this time (Fig. 5b), a result that follows from increasing crystallinity (and decreasing solubility) of gibbsite and kaolin in the soil (DiChiaro, 1998, see also the range in pK_{diss} values in Eq. (6a)).

A predominance diagram (Fig. 5c) shows that chronosequence soil solutions migrate from smectite to kaolinite and finally to gibbsite stability fields with increasing soil age. Although the youngest soil plots in the smectite stability field (because of high pH), no smectite was found in this soil, which emphasizes the important kinetic limitations to mineral formation (see Section 3). Furthermore, Fig. 5c shows that the precise location of the lines separating the stability domains depends upon the crystallinity of the two participating solids (subscripts WC and PC refer to well-crystallized and poorly crystallized phases, respectively). Two of the four possible lines separating kaolinite and gibbsite are shown here to illustrate the fact that soil solutions from the four oldest soils fall into either kaolinite or gibbsite stability fields, depending on the solubility data employed in the thermodynamic calculations. This range in solubility characteristics that follows from a corresponding range in crystallinity is termed the solubility "window" for a given mineral (Sposito, 1994) and it underlines the

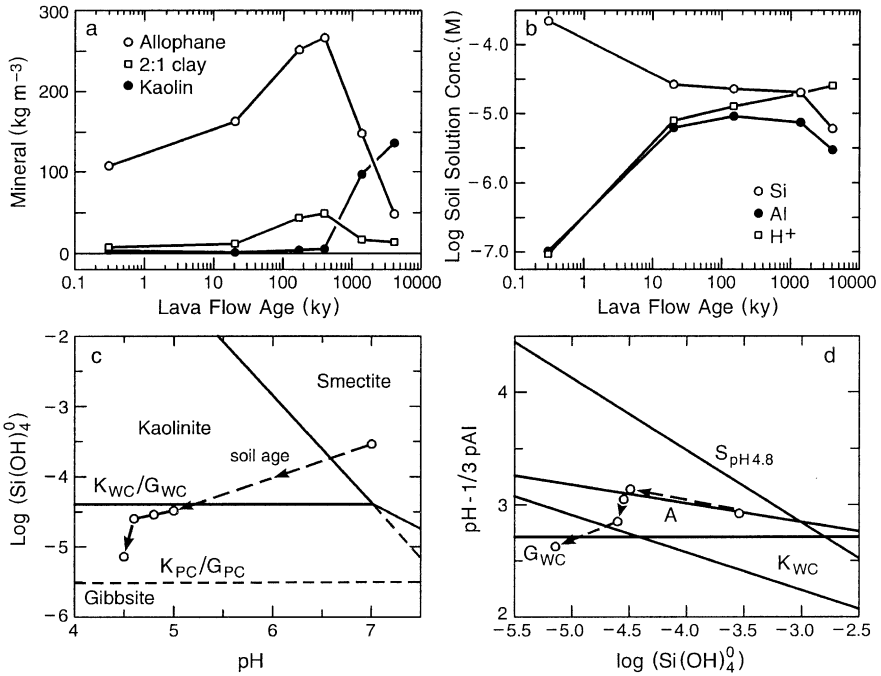

Fig. 5. Change of soil–mineral and soil–solution properties along a chonosequence sampled at 2500 mm of rainfall in Hawaii (Vitousek et al., 1997; Chadwick et al., 1999; Chorover et al., 1999). Quantified mineral composition (a) plotted from data contained in Vitousek et al. (1997) and Chorover et al. (1999). Soil solution composition (b) plotted from lysimeter data (Lars Hedin, unpubl. data). Plots (c) and (d) are solubility and predominance diagrams for mineral phases potentially controlling silica and aluminum activities in soil solutions. Data points for soil solutions in the Hawaiian chronosequence are plotted on both graphs. The smecite is a beidellite. Graphs were generated assuming log $(Fe^{3+}) = -11$ (equilibrium with ferrihydrite), log $(Mg^{2+}) = -4$, and water and solid activities are unity. The symbols G, K, S and A refer to gibbsite, kaolinite, smectite and proto-imogolite allophane, respectively. The subscripts PC and WC refer to well-crystallized (less soluble) and poorly crystallized (more soluble) forms.

fact that such boundaries in natural soils are not clear-cut. In addition, these solubility windows indicate that coexistence of different minerals over a range in soil solution conditions is consistent with thermodynamics. Thus, a complex mineral assemblage may persist despite a change in pedogenic environment because of shifts in stability boundaries that accompany increasing crystallinity of constituent solid phases, a process known as Ostwald ripening (Steefel and Van Capellen, 1990).

Although not stable over the long-term relative to more crystalline phases, short-range-order solids can control the solubility of mineral-forming elements over pedogenically meaningful time periods. Fig. 5d shows that the soil solution chemistry data are consistent with Al and Si solubility control by proto-imogolite allophane during early stages of soil development, with older soils

plotting closer to the kaolinite and finally the gibbsite solubility lines. These equilibrium solubility calculations are indeed consistent with mineral transformations observed in the field sites (Fig. 5a). Allophane does not figure into predominance diagrams such as Fig. 5c because it is not favored thermodynamically over the other three solid phases under any of the conditions depicted. However, agreement between the solubility (Fig. 5d) and mineralogy (Fig. 5a) data underscore the important role of such metastable phases in affecting the rate of soil development. Inconsistencies between observed soil mineral composition and stability-field plots of solution chemistry data is evidence of kinetic limitations to mineral transformations (Lindsay, 1979). In theory, such discrepancies can be resolved through consideration of mineral transformation rates and Ostwald ripening processes (see also Section 3), but the requisite kinetic data are often lacking (Bethke, 1996).

2.3. Oxidation–reduction reactions

Along with soil solution pH, soil redox status (i.e., pe or Eh) is a master variable affecting the trajectory of pedogenesis. The capacity of the soil to buffer changes in redox status determines the rate and extent of soil morphological response to inputs of electrons (von der Kammer et al., 2000). Both biotic and abiotic soil processes result in electron transfer among soil constituents, with disequilibrium arising primarily from the incorporation of bioavailable, plant-derived reduced C compounds into soil (Fig. 1). The oxidation of organic matter (e.g., CH_2O) is coupled to one of several potential terminal electron acceptors present in soil (e.g., O_2, NO_3^-, Fe(III), Mn(IV), SO_4^{2-}, CO_2). While bioavailable organic matter constitutes the bulk of soil reduction capacity, the quantity of available electron acceptors is distributed among several important oxidizing agents whose total effective concentration represents the soil oxidation capacity, OXC(s) (Heron et al., 1994):

$$\mathrm{OXC(s)} = 4[\mathrm{O_2}] + 5[\mathrm{NO_3^-}] + 2[\mathrm{Mn(IV)}] + [\mathrm{Fe(III)}] + 8[\mathrm{SO_4^{2-}}] + 4[\mathrm{CH_2O}] \quad (10)$$

The meaning of OXC(s) is, therefore, analogous to ANC(s): brackets denote molar concentrations (mol m^{-3} soil), but here stoichiometric coefficients denote the moles of electrons transferred per mole of oxidizing agent in corresponding terminal electron accepting processes (TEAPs) as shown in Table 1 (Eqs. (R.1), (R.2), (R.3), (R.5), (R.8), and (R.10)). These reduction half reactions each represent different TEAPs that proceed in the forward direction when combined with the oxidation of organic matter (e.g., reverse of Table 1) to yield a complete exergonic redox reaction.

Possible redox reactions are dictated by the state of the soil system and the corresponding Gibbs energies of reaction. Among the reactions that are possible

Table 1
Selected reduction half-reactions important in soils[a]

Reaction	log K
(R.1) $1/4\ O_2\ (g)+H^+\ (aq)+e^-\ (aq)=1/2\ H_2O\ (l)$	20.75
(R.2) $1/5\ NO_3^-\ (aq)+6/5\ H^+\ (aq)+e^-\ (aq)=1/10\ N_2\ (g)+3/5\ H_2O\ (l)$	21.05
(R.3) $1/2\ MnO_2\ (s)+2H^+\ (aq)+e^-\ (aq)=1/2\ Mn^{2+}\ (aq)+H_2O\ (l)$	20.85
(R.4) $1/2\ NO_3^-\ (aq)+H^+\ (aq)+e^-\ (aq)=1/2\ NO_2^-\ (aq)+1/2\ H_2O\ (l)$	14.15
(R.5) $Fe(OH)_3\ (s)+3\ H^+\ (aq)+e^-\ (aq)=Fe^{2+}\ (aq)+3\ H_2O\ (l)$	17.92
(R.6) $Fe^{3+}\ (aq)+e^-\ (aq)=Fe^{2+}\ (aq)$	12.05
(R.7) $1/2\ O_2\ (g)+H^+\ (aq)+e^-\ (aq)=1/2\ H_2O_2\ (aq)$	11.56
(R.8) $1/8\ SO_4^{2-}\ (aq)+5/4\ H^+\ (aq)+e^-\ (aq)=1/8\ H_2S\ (g)+1/2\ H_2O\ (l)$	5.13
(R.9) $1/2\ CH_2O\ (aq)+H^+\ (aq)+e^-\ (aq)=1/2\ CH_3OH\ (aq)$	3.99
(R.10) $1/4\ CH_2O\ (aq)+H^+\ (aq)+e^-\ (aq)=1/4\ CH_4\ (g)+1/4\ H_2O\ (l)$	6.94
(R.11) $1/8\ CO_2\ (g)+H^+\ (aq)+e^-\ (aq)=1/8\ CH_4\ (g)+1/4\ H_2O\ (l)$	2.87
(R.12) $H^+\ (aq)+e^-\ (aq)=1/2\ H_2\ (g)$	0.00
(R.13) $1/4\ CO_2\ (g)+H^+\ (aq)+e^-\ (aq)=1/4\ CH_2O\ (g)+1/4\ H_2O\ (l)$	−1.20

[a]Data from Stumm and Morgan (1996) and Bartlett and James (1993) for 25°C.

thermodynamically, those that predominate at any given point in time are determined by redox kinetics, the latter being governed to a large degree by soil microbial catalysis (Fenchel et al., 1998). A sequence of TEAPs is observed typically along pe gradients both spatially and temporally in soil systems (Patrick and Henderson, 1981; Patrick and Jugsujinda, 1992). This sequence corresponds closely to progressive decreases in the Gibbs energy of the full redox reaction. Fig. 6 shows this sequence of reactions for a hypothetical soil containing a finite supply of bioavailable organic matter and soil oxidation

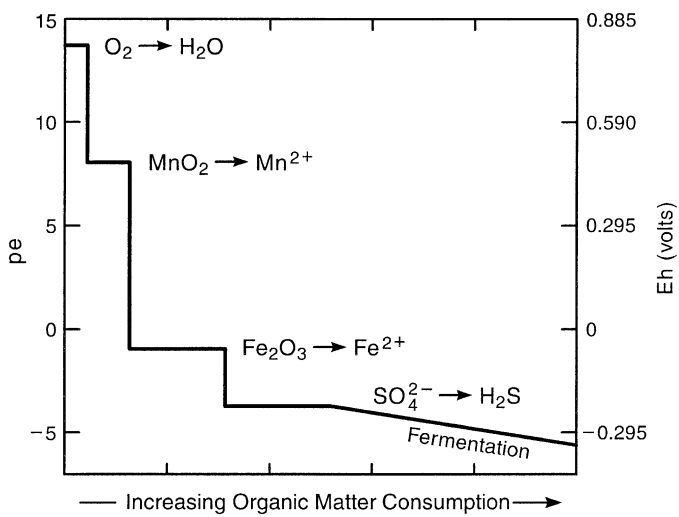

Fig. 6. A hypothetical plot showing change in terminal electron accepting processes for a soil containing a finite supply of bioavailable organic matter and soil oxidation capacity (after Scott and Morgan, 1990).

capacity (modified from Scott and Morgan, 1990). Since O_2 is sparingly soluble in water (0.25 mM at 25°C) it can be depleted rapidly by microbial and root respiration in soils subjected to limited influx of air or oxygenated water. When that occurs, dissolved nitrate and available Mn(IV) solids are utilized as alternative electron acceptors during oxidation of OM (denitrification, Eq. (R.2) and Mn reduction, Eq. (R.3), in Table 1). As these reactants become depleted, further reduction in pe (Eh) results in the successive use of Fe(III) solids (ferric reduction, Eqs. (R.5–R.6)), SO_4^{2-} (sulfate reduction, Eq. (R.8)), and eventually organic matter itself (fermentation, Eq. (R.9)) or CO_2 (methanogenesis, Eq. (R.11)) (Table 1). In each case, depletion of reactant oxidizing agents and accumulation of their reduced-form products (e.g., Mn^{2+}, Fe^{2+}, HS^-, CH_3COO^-) diminishes the energy yield of a given TEAP as the Gibbs energy for the full reaction approaches zero (equilibrium). Reduced Fe^{2+} and Mn^{2+} are more soluble than their oxidized counterparts, and their removal from the soil by leaching results in a permanent loss in OXC(s). As catalysts, microorganisms can affect the rate of these reactions, but they cannot alter the energy yield, which is governed by thermodynamics. The energetics (ΔG_r) can be computed from Eq. (9), given log K data such as those in Table 1, along with known activities of the participating chemical species (redox couples) and pH.

Assessment of the redox status of soils involves the measurement of Eh by platinum electrode, its computation based on the chemical analysis of the main redox couples, or the use of indicator dyes (Bartlett and James, 1993, 1995). The three methods often show poor agreement (Lindberg and Runnells, 1984), and this is attributed to (1) misbehavior of the Pt electrode, (2) slow kinetics of most redox couple reactions and resultant disequilibrium among different redox couples in the same system, and (3) the existence of mixed potentials in natural waters (Langmuir, 1997). Stable Eh measurements are only possible in well-poised systems, which have a high redox capacity to buffer changes in Eh. The redox capacity, which is complementary to OXC(s), may be defined as the moles of reductant e^- charge required to lower the Eh of a fixed volume of soil by 1.0 V (Nightingale, 1958). High redox capacity or OXC(s) is expected to confer stability to redox-induced pedogenic processes such as Mn and Fe reduction.

Soils can have high OXC(s) because of high throughflux of oxygenated water, a high concentration of alternative electron acceptors, or both (Eq. (10)). An open soil system can remain oxic despite large inputs of reduced C. However, spatial and temporal heterogeneity in redox status is great in many humid zone soils because of the coexistence of (1) transient water saturation, (2) O_2 diffusion limitations, (3) high inputs of reductant and (4) high microbial biomass concentrations (Fiedler, 2000; Teichert et al., 2000). These characteristics can lead to rapid local fluctuations in soil Eh and disequilibrium among redox couples. For example at the soil ped scale, O_2 depletion and denitrification is observed within soil aggregates in a soil system that is oxic overall

(Sexstone et al., 1985). This variability in redox status bears heavily on soil weathering and morphology. Dissimilatory, reductive dissolution of Fe(III) and Mn(IV) hydroxides gives rise to mottling and gleying, among other redoximorphic features (Lovley, 2000). The rapid fluctuations in redox state combined with problems in measurement Eh status have made it difficult to measure redox driven pedogenesis in action. Usually it is the gleyed horizon or iron mottles that provide the evidence for reducing conditions, and from these it is difficult to interpret the longevity of a particular Eh condition much less the sequence of reactions.

Iron reduction–oxidation delineates an important redox threshold in pedogenesis that is illustrated cogently in a climate sequence on the island of Maui in Hawaii (Fig. 7). Fig. 7a shows the decrease in Eh, measured by platinum electrode, that corresponds to an increase in mean annual rainfall. These Eh values represent mixed potentials in a non-equilibrium soil system and they must be interpreted cautiously (Bartlett and James, 1993), but the Pt electrode does respond better to the Fe^{3+}–Fe^{2+} redox couple than to many others (McBride, 1994). For this reason, a threshold decrease in ferric hydroxides (dominated in the Maui soils by poorly crystalline ferrihydrite) is observed as soil Eh drops below 330 mV (Fig. 7b). According to Eq. (R.5) in Table 1, at 330 mV the ferrihydrite–Fe^{2+} (aq) equilibrium is defined by $pFe^{2+}–pH = 1.5$. Therefore, for a soil pH of 4.5, sustaining Fe^{2+} concentrations of less than 1 $\mu mol\ l^{-1}$ will continue to drive the reductive dissolution of ferrihydrite until it is completely removed from the soil profile. Indeed, sub-micromolar concentrations of Fe^{2+} are maintained by the high leaching rates observed at this point in the climosequence (> 3 m of rainfall, Fig. 7a). The removal of Fe(III) hydroxides is a pedogenic threshold that can strongly impact ecosystem processes such as phosphate retention (Fig. 7c), with consequences for the biota that may feed back to affect soil development (Miller et al., 2001).

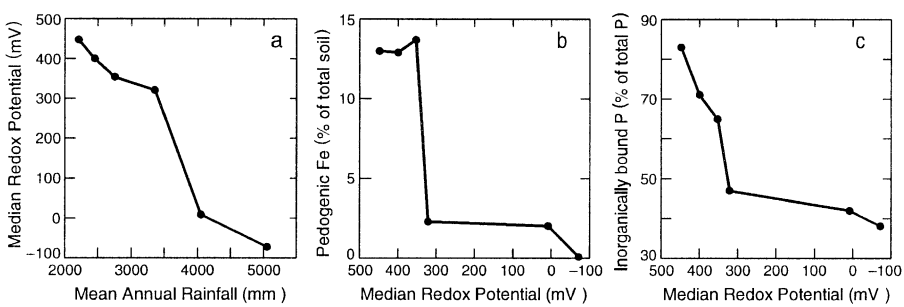

Fig. 7. The control of long-term average redox potential (360 platinum electrode measurements taken every 6 weeks over 18 months) on pedogenic Fe (pyrophosphate, oxalate, and dithionite–citrate extracts) and inorganic levels of P (modified Hedley fractionation) in upland soils sampled on a 400 ka lava flow along a climosequence ranging from 2200 to 5000 mm of rainfall (Schuur et al., 2001; Miller et al., 2001).

Full redox reactions (i.e., coupling of organic matter oxidation with a given TEAP) result in either net production or consumption of protons, depending upon the ratio of H^+ to e^- in the sum of oxidation and reduction half reactions (Table 1). Proton deficit or surplus sets up chemical gradients that feed into the acid–base reactions discussed previously. For example, nitrification (NH_4^+ oxidation) and sulfide oxidation result in net proton production, whereas denitrification, dissimilatory Fe reduction and sulfate reduction are generally proton consuming reactions. In addition to effects on soil acidity, changes in redox state can shift the soil system among mineral stability fields, but the pedogenic outcome is strongly dependent on fluxes of water and solutes (Lerman, 1990). For example, the reductive dissolution of Fe(III) and Mn(IV) solids that occurs under suboxic conditions can lead to formation of Mn(II) and Fe(II) solids (e.g., $MnCO_3$, $FeCO_3$, $Fe(OH)_2$) when water fluxes are low relative to (hydr)oxide dissolution rates (Schwertmann and Taylor, 1989; McKenzie, 1989). Alternatively, high water flux can prevent precipitation by maintaining solutions below saturation limits ($\Omega < 1$) as in the case of the Maui climate sequence discussed above, or by affecting the kinetics of nucleation (Lasaga, 1998). In either case, the result is more efficient removal of these lithogenic metals from the soil profile.

3. Kinetic constraints on threshold behavior

Since soils are open systems, the leaching of reaction products (Fig. 1) affects the degree to which dissolution products accumulate and secondary solids precipitate. Although a weathering reaction may be spontaneous from the perspective of thermodynamics, it may be sufficiently slow (e.g., quartz dissolution) to be negligible in comparison to more rapid reactions (e.g., olivine, amphibole and feldspar dissolution), even when extended over the long time scales of pedogenesis. The same is true for precipitation reactions; despite supersaturation ($\Omega > 1$), the rate of nucleation and precipitation of secondary solid phases (time scales ranging from days to years) may be slower than the efflux of supersaturated solution (Lerman, 1990; Lasaga, 1998).

Adsorption/desorption reactions (ion exchange, surface complexation) govern base cation saturation of the exchange complex and exchangeable acidity. These reactions are relatively rapid (time scales ranging from microseconds to hours) when they occur on accessible surfaces, but a slow approach to equilibrium (months to years) is observed when intraparticle or surface diffusion is rate limiting (Scheidegger and Sparks, 1996). Surface processes, along with rapidly dissolving solids (carbonates, salts and amorphous minerals), regulate the short-term composition of soil solution that unfolds, for example, during large infiltration events. Still, on a long-term basis, it is the slower dissolution and precipitation reactions involving the solid phase that resupply the adsorptive

species and ultimately regulate soil solution composition. Given the large range in time scales characteristic of soil chemical processes, (Amacher, 1991) conceptual models treat all or some of the pertinent reactions as kinetically limited. On the time scales of both water transport and soil development, aqueous speciation and surface reactions (adsorption–desorption) are often modeled as equilibrium processes, whereas precipitation–dissolution and heterogeneous redox reactions must be considered as rate-limited (Furrer et al., 1989; Robarge and Johnson, 1992; Suarez and Goldberg, 1994; Yeh et al., 1995).

Rock minerals dissolve at widely varying rates depending on their respective resistances to chemical weathering (Fig. 8). Weathering resistance is determined by the degree of Si—O—Si bonding (Brantley and Chen, 1995) and ligand exchange kinetics of the mineral-derived cations (Casey and Ludwig, 1995). Therefore, minerals with isolated Si tetrahedra that are bonded through other cations have low molar Si/O ratios, low numbers of bridging oxygens per Si tetrahedron, and weather most rapidly (e.g. olivine), whereas chain, sheet and framework structures exhibit increasing Si/O ratio and hence, increased resistance and slower dissolution kinetics (Fig. 8). Weathering in such a multicomponent system is represented by a set of parallel reactions (cf. Eqs. (2), (3a,b) and (4)) comprising several different reactant solids. Soil dissolution will be dominated by the phases for which the product of (i) surface-normalized rate (e.g., moles of mineral dissolved per square meter of mineral surface per second) and

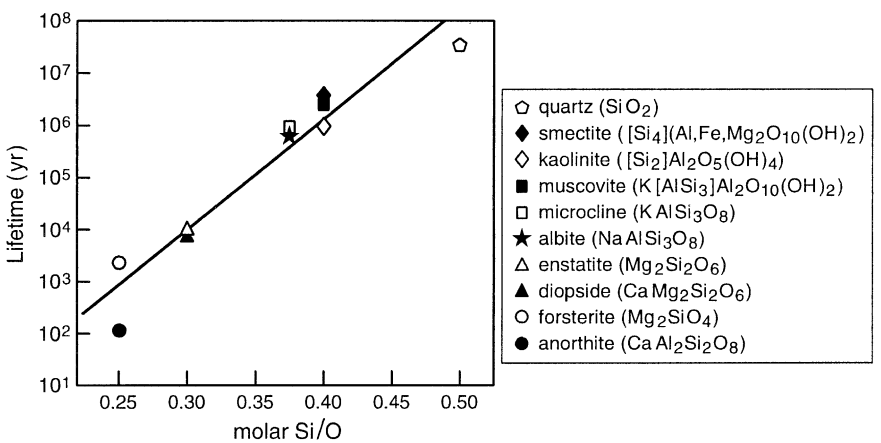

Fig. 8. The time in years required to dissolve a 1 mm equivalent diameter crystal for different classes of silicate minerals at 25°C, pH 5, and far from equilibrium versus the molar ratio of silicon to oxygen in the structure. For sheet silicates, only tetrahedral sheet oxygens are considered. Calculation of lifetime is according to Lasaga (1998); $t_{\text{lifetime}} = r_0(kV)^{-1}$, where r_0 is the initial radius (m) of the crystal (assumed to be spherical), k is the dissolution rate constant (mol m^{-2} $year^{-1}$), and V is the molar volume of the mineral (m^3 mol^{-1}). Sources of rate data: quartz, Rimstidt and Barnes (1980); smectite, Furrer et al. (1993); kaolinite, Wieland and Stumm (1992) and Nagy (1995); muscovite, Lin and Clemency (1981); microline and albite, Blum and Stillings (1995); enstatite and diopside, Brantley and Chen (1995); forsterite, Lasaga (1998).

(ii) reactive surface area (e.g., square meters of mineral surface per cubic meter of soil) is greatest. Thus, in accordance with Fig. 8, weathering in fresh rock far from equilibrium should be dominated by dissolution of olivines, selected amphiboles and pyroxenes, whereas micas and some feldspars, which exhibit slower rates of dissolution, will predominate once these easily weathered phases are depleted.

Since each mineral weathering reaction represents a unique stoichiometry and is subject to different degrees of congruency, tendencies toward secondary mineral formation and solute release will likewise be distinct. For example, weathering reactions involving low Si/O ratio minerals are strongly congruent leading to supersaturation of solution with respect to short-range-ordered minerals (e.g., allophane) whose precipitation confers metastability prior to the formation of more crystalline secondary phases (Steefel and Van Capellen, 1990). In contrast, weathering reactions involving mica are strongly incongruent leading to rapid formation of well-crystallized secondary minerals such as vermiculite, smectite and kaolinite. Feldspars fall into an intermediate category because they are framework silicates that can weather congruently along their edges, but they can also undergo incongruent weathering leading to isovolumetric replacement by secondary minerals (Nahon, 1991).

3.1. Mineral dissolution rates

Although mass action equations, such as Eqs. (2), (3a,b), (4), can be used to determine the degree of solution saturation with respect to a given mineral phase, they are independent of reaction mechanism and their utility in predicting dissolution rates is limited. Significant research has been conducted since the 1960s to elucidate the kinetics and mechanisms of dissolution and precipitation at the molecular scale. The surface reaction hypothesis asserts that the dissolution of most slightly soluble oxides and silicates is controlled by chemical processes at the mineral surface (Stumm and Wollast, 1990; Stumm, 1992). The common observation of steady-state dissolution rates for laboratory systems far from equilibrium (e.g., Furrer and Stumm, 1986; Banwart et al., 1989; Bloom and Erich, 1987; Dove and Crerar, 1990) is consistent with a surface-detachment mechanism as the rate limiting step. Specifically, the adsorption of protons and metal-complexing ligands at mineral surfaces is thought to result in the polarization of metal–oxygen bonds in the solid, with the rate-limiting step being the detachment of an aquometal or ligand–metal complex. Corresponding rate laws for proton and ligand promoted dissolution may be written as:

$$R_{\mathrm{H}} = k_{\mathrm{H}} C_{\mathrm{H,S}}^{n} (\mathrm{mol\,m^{-2}s^{-1}}) \tag{11a}$$

$$R_{\mathrm{L}} = k_{\mathrm{L}} C_{\mathrm{L,S}} (\mathrm{mol\,m^{-2}}s^{-1}) \tag{11b}$$

where R_H and R_L are the rates of proton and ligand promoted dissolution, respectively, k_H and k_L are first order rate coefficients, $C_{H,S}$ is the surface proton concentration and $C_{L,S}$ is the concentration of adsorbed ligands (e.g., oxalate, succinate, hydroxide). The value of n in Eq. (11a) corresponds to the valence of the metal released from the solid (e.g., $n = 2$ for BeO, $n = 3$ for Al_2O_3) (Furrer and Stumm, 1986). This integer dependence on adsorbed proton concentration is in contrast to fractional order dependence with respect to bulk H^+ concentration (Lasaga, 1998). Since mineral dissolution correlates with net adsorption of H^+, OH^- and other bond polarizing ligands, mineral dissolution rate is often found to be minimum at the point of zero net proton charge (PZNPC; pH value where net proton adsorption is zero), and to increase at pH values both above and below the PZNPC (Stumm, 1992; Sposito, 1994).

Transferring this concept to heterogeneous mineral assemblages that occur in soils is nontrivial. However, it has been observed that highly weathered tropical soils evolve to a minimal surface charge and that element release increases significantly at both higher and lower pH values (Chorover and Sposito, 1995a,b). The rate of mineral dissolution, expressed in terms of mass loss per unit reactive surface area and time, is equal to $R_H + R_L$ (Eqs. (11a,b)) only when back reactions are negligible. A significant decrease in the dissolution rate occurs when reaction products accumulate and equilibrium is approached. In soil profiles, maximum rates occur in horizons where most products are eluviated such as E horizons, but they plummet in illuvial Bt and Bs horizons. Furthermore, White et al. (1996) showed that surface-normalized dissolution rate constants for individual primary minerals decrease with increasing soil age, suggesting that the density of reactive, high-energy surface sites may be diminished over long-term weathering in the natural environment. Taken together, these factors confer stability against further weathering-induced transformation, thereby attenuating a threshold response.

Comparison of soil weathering rates measured in the laboratory and estimates derived from field-based studies indicate that laboratory rates are one to four orders of magnitude greater than field estimates (Schnoor, 1990; Asolekar et al., 1991; Swodoba-Colberg and Drever, 1993; Velbel, 1993; Sverdrup and Warfvinge, 1995; White et al., 1996). For example, based on measures of dissolved silica as a conservative tracer of weathering in the B horizon of a forest soil, laboratory rates are approximately 10^{-12} to 10^{-11} mol m^{-2} s^{-1}, while field rates are 10^{-14} to 10^{-12} mol m^{-2} s^{-1} (Schnoor, 1990). This discrepancy is observed commonly and attributed to the difficulty of estimating a reactive surface area of field soil minerals and to macropore water flow in structured field soils. Indeed, the distribution of pore sizes in soils gives rise to highly variable water flux rates at the micro scale. Depending on the degree of mixing of soil solution between micro and macropores, distinctly different aqueous geochemical environments may occur in different sized pores, with smaller pores (slower water percolation) permitting a greater build-up of reaction

products, which promotes the formation of secondary minerals (Lasaga, 1998; Nahon, 1991). Furthermore, laboratory studies have shown that short-time element release corresponds to ion exchange reactions and that steady-state mineral dissolution proceeds after this threshold removal of cations (Schnoor, 1990; van Grinsven and van Riemsdijk, 1992; Dahlgren and Walker, 1993). In natural systems, the wide variety of pore sizes and water flux leads to a complex mosaic of ion exchange and mineral dissolution reactions that is spatially variable within a profile.

3.2. Neoformation of secondary phases

In contrast to dissolution, in which kinetics of element release are controlled by parallel dissolution reactions dominated by the more rapidly dissolving solid phases, precipitation of secondary minerals proceeds in series according to Ostwald's Step Rule. This rule states that a thermodynamically unstable mineral reacts over time to form a sequence of progressively more stable minerals (Morse and Casey, 1988; Steefel and Van Capellen, 1990; Bethke, 1996). If the soil solution is oversaturated ($\Omega > 1$) with respect to several solid phases, the solid that forms first will be the one for which the value of $\Omega > 1$ is closest to unity. The remaining accessible solid phases form in order of decreasing solubility, with a corresponding decrease in their rate of formation. This decrease in formation kinetics with decreasing solid-phase solubility is attributed to a corresponding increase in interfacial Gibbs energy (i.e., the energy required to create the new surface) (Stumm, 1992).

As a result, poorly crystalline colloids with high specific surface areas and solubilities (e.g., allophane, ferrihydrite) are often the first to precipitate from supersaturated solutions, even though they may not be most stable thermodynamically (Morse and Casey, 1988; Steefel and Van Capellen, 1990). As the Ω value for the short-range-order phase is progressively diminished to unity, Ostwald ripening (dehydration with subsequent increase in crystallinity) leads to its transformation to more crystalline (less soluble) phases. In Fig. 4b, for example, given a solution with silicic acid activity equal to $10^{-3.5}$, we expect that allophane will precipitate first, followed by smectite, gibbsite and kaolinite, the latter remaining as most stable at pH 6.0 and constant silicic acid activity. Ostwald ripening also occurs within a single mineral type (e.g. kaolinite or gibbsite) if variable crystallinity confers a solubility range or "window" (e.g., Fig. 5c). Since soils are open systems, even intermediate ("metastable") phases may be maintained indefinitely (Sposito, 1994).

3.3. Water flux and solute removal

The amount and timing of water flux determines the rate and trajectory of soil evolution, since it carries reactants into the profile and contributes to down-

gradient transport of solute and colloidal products (Fig. 1). Water flux couples with reaction kinetics to control the distance from source to sink for soluble and colloidal reaction products. The degree of soil solution saturation (Ω) with respect to a given secondary mineral phase will tend to increase with increasing rate of precursor mineral dissolution, but will decrease as increasing water flux leaches solutes. Extensive leaching promotes a deep penetration of freshwater that depletes the profile mass of water-soluble species (e.g., comprising Si, Ca, Mg, K and Na), whereas less soluble elements (e.g., Al, Fe, Ti) and biogenic C and N are enriched preferentially. Conversely, at low water flux even soluble constituents can accumulate in solid-phase weathering products (e.g., carbonates, opaline silica) close in proximity to the parent material source. Therefore, precipitation and potential evapotranspiration, are critical determinants of pedogenesis.

The role of effective moisture (precipitation minus evapotranspiration) in developing soil properties has been studied intensively (Birkeland, 1999). Early soil classifications focused on zonal soils or the characteristic soil for a particular climate zone (Baldwin et al., 1938; Cline, 1949), and modern soil classifications use climate at several categorical levels (Soil Survey Staff, 1999). It is often difficult to sample a large number of sites along a climatic gradient in order to determine the changes in profile properties that follow from relatively small changes in climatic conditions. The Hawaiian Islands provide a unique opportunity to overcome this problem because same age lava flows can be followed for long distances through a number of different climate zones. To investigate the importance of differences in effective moisture in producing thresholds associated with changing leaching intensity, we utilize data from a climosequence ranging from 160 to 3000 mm of annual rainfall on a 170,000-year-old lava flow in Hawaii (Chadwick et al., 1994; Hsieh et al., 1998; Kelly et al., 1998). Soil profiles can be separated into those that receive < 1400 mm of rain and have an annual water deficit and those that have an annual surplus (Fig. 9a). In Fig. 9b, the ratio V/Vo is a measure of leaching intensity indexed at 1-m depth where V is the average annual depth of water penetration based on the effective annual moisture as shown in Fig. 9a and Vo is the total porosity minus the pores filled with bound water (< -1500 kPa) in the top meter. Use of V/Vo as an indicator of leaching intensity provides a measure of effective moisture that has been corrected for evapotranspiration and soil properties that affect porosity such as rock fragments and bulk density. When $V/\mathrm{Vo} = 1$ there is just enough water annually to completely fill the pores in the top meter. When $V/\mathrm{Vo} = 2$ all pores will be completely flushed.

In this case, $V/\mathrm{Vo} = 1$ occurs at about 1400 mm (Fig. 9b) and greater leaching intensity (V/Vo between 1 and 2) leads to a dramatic change in base cation saturation of the exchange complex (Fig. 9c). As rainfall increases along the climosequence the depth-weighted (1 m) average base saturation remains $> 90\%$ until leaching begins to occur during some period of the year. When

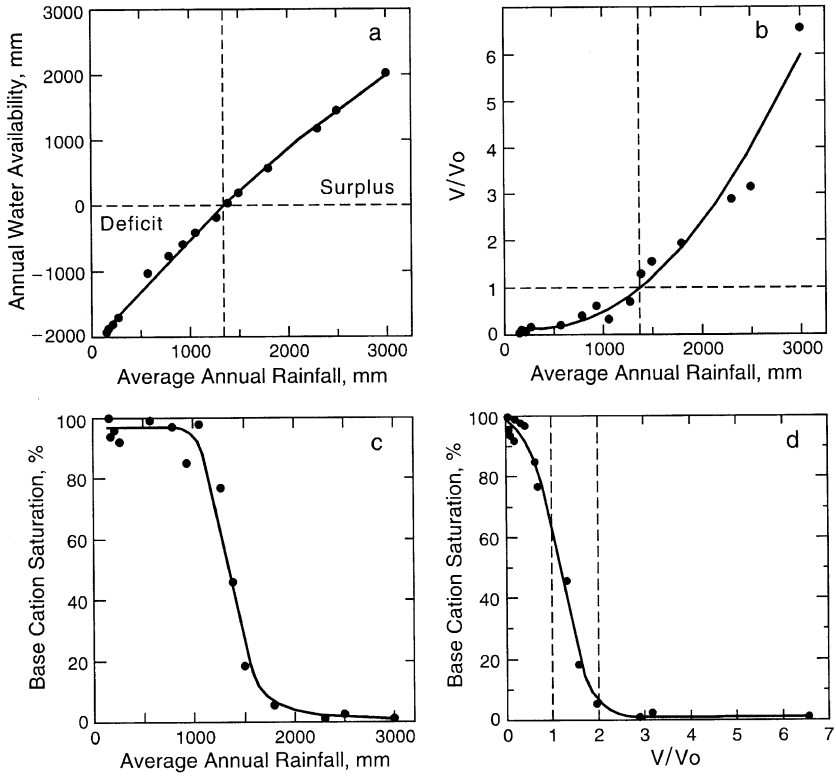

Fig. 9. Quantification of the leaching intensity as a function of increased rainfall and changed soil porosity sampled on a 170 ka lava flow along a climosequence ranging from 160 to 3000 mm of rainfall. Annual water balance (a) calculated based on procedures described by Arkley (1963), based on monthly rainfall values and daily pan evaporation data (Giambelluca et al., 1986), and integrated over a year to determine the degree of deficit or surplus for each rainfall site. Annual pore volumes of water (b); the values for V/Vo is a measure of leaching intensity indexed at 1-m depth, where V is the average annual depth of water penetration based on values from (a) and Vo is the available-water porosity in the top meter. Depth-weighted average base cation saturation as a function of rainfall (c) and leaching intensity (d) plotted from data in Chadwick et al. (1994), Kelly et al. (1998) and Stewart et al. (2001).

leaching reaches one to two pore volumes of water, there is a rapid loss of adsorbed base cations (and a parallel rise in exchangeable Al) and soils with $V/\mathrm{Vo} \sim 2$ have base saturation of $< 10\%$. Thus, a small increase in rainfall leads to a threshold that follows a pattern similar to that shown in Fig. 2 except that now it is effective moisture rather than time that is creating the proton rich environment. Soil profiles with values of $V/\mathrm{Vo} > 2$ show only minor differences in base saturation and pH because they all are being buffered by Al hydrolysis. Although the climosequence is sampled along the same age lava flow, there is a time-dependence to the leaching impact. Initial weathering rates were most rapid at the highest values of V/Vo, but they declined precipitously

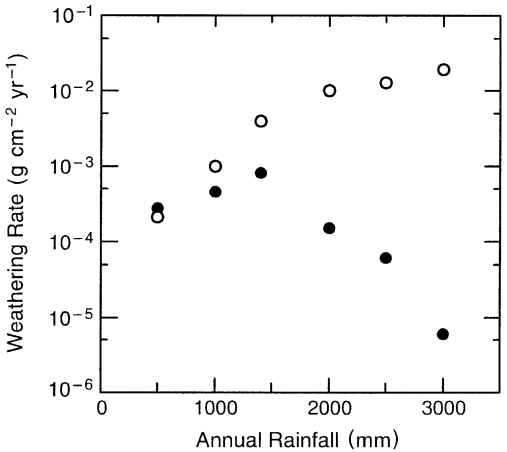

Fig. 10. Initial (open circles) and present-day (filled circles) weathering rates as a function of rainfall. Weathering rates are for Sr containing minerals in the Hawaiian lavas such as plagioclase feldspar. The weathering rate calculation is based on the $^{87}Sr/^{86}Sr$ isotopic ratio of exchangeable Sr and endmember contributions from lava weathering and rainwater (data are replotted from Stewart et al., 2001).

as all the primary minerals were depleted (at the highest rainfall sites first). Present day weathering rates at the high rainfall sites are actually lower than rates prevailing at sites receiving less moisture because of the depletion of primary minerals (Fig. 10) (Stewart et al., 2001). A climosequence on a younger lava flow would probably have its base cation saturation threshold at higher rainfall and V/Vo values because of the greater buffering capacity afforded by higher contents of primary silicate minerals in the younger soils. Soil profiles can exist in different thermodynamically stable states at different times. In this case as in many, it is the kinetics of the system—specifically, the coupling of moisture flux with mineral transformation rates—that determines the properties of each profile along the climosequence.

4. Conclusions

Soils are open systems that act as a membrane at Earth's surface. Water and dissolved acids are the main materials transferred into soils, whereas water and lithogenic solutes dominate the output with the net result being depletion of rock-forming constituents such as silica and base cations. The time-dependent coupling of water flux and chemical reactions determines the nature of the critically important residual products. Pedogenesis is a biogeochemical process that is constrained by thermodynamics, but still maintains considerable flexibility as a result of parallel reaction kinetics, and a spatially heterogeneous matrix. In the open system, there are many processes that are governed by nonlinear response to changes in environmental variables and/or internal soil properties.

From a thermodynamic perspective, the chemistry of pedogenesis is characterized by a number of thresholds. Over time, the reaction of atmospheric acids with soil bases changes the acid neutralizing capacity of soil to an extent that is controlled by the prevailing buffering reactions. The amount of proton consumption and its effect on pH depend on the nature of the reactive species, their relative amounts, and their respective rates of reaction. Ion exchange and surface complexation reactions consume protons in the short-term, but long-term buffering derives from mineral weathering. Mineral dissolution reactions occur in parallel. Therefore, at any point in time, those minerals that exert the greatest control on solution chemistry will be those for which the product of (1) surface-normalized dissolution rate and (2) reactive surface area is highest. Although values for these parameters may be obtained readily in laboratory studies of mineral specimens, they are more difficult to quantify for the complex mineral assemblages that occur in soils. Furthermore, a range in solubility (and crystallinity) characteristics for a given mineral likely occurs within the same soil. This should subdue stability boundaries and temper thresholds in mineral transition that must be traversed during soil development. In so far as element solubility is affected by redox fluctuations, removal and/or translocation of redox sensitive elements in impacted soil profiles depends on the rate of energetically favorable reactions and the efflux of solutes in percolating water. The conditions favorable to threshold response are best revealed by high-resolution studies across environmental gradients. For example, the stepwise nature of terminal electron accepting processes is manifest as a threshold release of Fe from soil profiles when the weathering environment crosses a relatively narrow stability boundary for this redox active metal.

Threshold response is attenuated when the reaction kinetics and removal of products are sufficiently slow, such as when the buffering capacity is large relative to reactant inputs. Examples include the weathering of a base-cation rich basalt in an arid climate or the buffering of reductant input by a well-poised soil redox system. In addition, prior weathering regimes can preclude mineralogical transformations that might otherwise be expected for a specific set of climatological/biological state factors acting on a given parent material. Although previously labeled pedogenic “inertia”, this behavior is predictable from considerations of mineral stability in the context of soil development; it underlines the boundary conditions that prior weathering regimes impose on subsequent pedogenic responses.

Although equilibrium calculations for soil systems readily produce stability fields and thresholds between them, discrepancies between predicted and measured system composition occur because of kinetic limitations and spatial disequilibrium within soils. As a result, parallel reactions predominate over serial reactions. Hydraulic mixing between micro-, meso- and macro-porous domains is incomplete, which leads to locally distinct aqueous geochemical environments. In addition, short-term temporal changes in water saturation/so-

lute concentrations and influx (or efflux) of reactants (or products) and energy is variable in time and space. Added to the myriad chemical environments and variable environmental forcing agents is a serious problem in applying appropriate sampling techniques. Novel sampling and analytical techniques are required to better characterize the biogeochemical heterogeneity presented by a soil profile.

Acknowledgements

We benefited greatly from discussions with Bob Gavenda, Chris Smith, Goro Uehara, Milan Pavich, Eugene Kelly, Peter Vitousek, Jennifer Harden, and Bob Graham, and received helpful manuscript reviews from Alex McBratney, Alfred Hartemink, Don Sparks, Peter Vitousek and Nico van Breemen. This work was supported by grants to OAC from the Andrew Mellon Foundation and the NSF Environmental Geochemistry and Biogeochemistry program and to JC from the USDA Program 25.0 in Soils and Soil Biology (# 97-35107-4360) and the Andrew Mellon Foundation. The USDA Natural Resource Conservation Service (Chris Smith and Bob Gavenda) provided much needed logistical support for our field sampling in Hawaii.

References

Amacher, M.C., 1991. Methods of obtaining and analyzing kinetic data. In: Sparks, D.L., Suarez, D.L. (Eds.), Rates of Soil Chemical Processes. SSSA Spec. Publ., vol. 27, Soil Sci. Soc. Am, Madison, WI, pp. 19–59.

Arkley, R.J., 1963. Calculation of carbonate and water movement in soil from climate data. Soil Sci. 96, 239–248.

Asolekar, S.R., Valentine, R.L., Schnoor, J.L., 1991. Kinetics of chemical weathering in B horizon Spodosol fractions. Water Resour. Res. 27, 527–532.

Baldwin, M., Kellogg, C.E., Thorp, J., 1938. Soil Classification. Soils and Men. USDA Yearbook, U.S. Government Printing Office, Washington, DC, pp. 979–1002.

Banwart, S., Davies, S., Stumm, W., 1989. The role of oxalate in accelerating the reductive dissolution of hematite by ascorbate. Colloid Surf. 39, 303–309.

Bartlett, R.J., James, B.R., 1993. Redox chemistry of soils. Adv. Agron. 50, 151–208.

Bartlett, R.J., James, B.R., 1995. System for categorizing soil redox status by chemical field testing. Geoderma 68, 211–218.

Bethke, C.M., 1996. Geochemical Reaction Modeling. Oxford Univ. Press, New York.

Birkeland, P.W., 1999. Soils and Geomorphology. Oxford Univ. Press, New York.

Bloom, P.R., Erich, M.S., 1987. Effect of solution composition on the rate and mechanism of gibbsite dissolution in acid solutions. Soil Sci. Soc. Am. J. 51, 1131–1136.

Blum, A.E., Stillings, L.L., 1995. Feldspar dissolution kinetics. In: White, A.F., Brantley, S.L. (Eds.), Chemical Weathering Rates of Silicate Minerals. Mineral. Soc. Am., Washington, DC, pp. 291–352.

Bockheim, J.G., 1980. Solution and use of chronofunctions in studying soil development. Geoderma 24, 71–85.

Brady, P.V., Walther, J.V., 1989. Controls on silicate dissolution rates in neutral and basic pH solutions at 25°C. Geochim. Cosmochim. Acta 53, 2823–2830.

Brantley, S.L., Chen, Y., 1995. Chemical weathering rates of pyroxenes and amphiboles. In: White, A.F., Brantley, S.L. (Eds.), Chemical Weathering Rates of Silicate Minerals. Reviews in Mineralogy, vol. 31, Mineralogical Society of America, Washington, DC.

Bryan, W.H., Teakle, L.J.H., 1949. Pedogenic inertia: a concept in soil science. Nature 164, 969.

Buol, S., Eswaran, H., 2000. Oxisols. Advances in Agronomy 68, 151–195.

Casey, W.H., Ludwig, C., 1995. Silicate mineral dissolution as a ligand exchange reaction. In: White, A.F., Brantley, S.L. (Eds.), Chemical Weathering Rates of Silicate Minerals. Reviews in Mineralogy, vol. 31, Mineralogical Society of America, Washington, DC.

Chadwick, O.A., Olson, C.G., Hendricks, D.M., Kelly, E.F., Gavenda, R.T., 1994. Quantifying climatic effects on mineral weathering and neoformation in Hawaii. Proc. 15th Int. Soil Sci. Congr. 8a, 94–105.

Chadwick, O.A., Nettleton, W.D., Staidl, G.J., 1995. Soil polygenesis as a function of quaternary climate change, Northern Great Basin, U.S.A. Geoderma 68, 1–26.

Chadwick, O.A., Derry, L.A., Vitousek, P.M., Huebert, B.M., Hedin, L.O., 1999. Changing sources of nutrients during four million years of ecosystem development. Nature 397, 491–497.

Chorover, J., Sposito, G., 1995a. Dissolution behavior of kaolinitic tropical soils. Geochim. Cosmochim. Acta 59, 3109–3121.

Chorover, J., Sposito, G., 1995b. Surface charge characteristics of kaolinitic tropical soils. Geochim. Cosmochim. Acta 59, 875–884.

Chorover, J., DiChiaro, M.J., Chadwick, O.A., 1999. Structural charge and cesium retention in a chronosequence of tephritic soils. Soil Sci. Soc. Am. J. 63, 169–177.

Cline, M.G., 1949. Basic principals of soil classification. Soil Sci. 67, 81–91.

Cronan, C.S., Walker, W.J., Bloom, P.R., 1986. Predicting aqueous aluminum concentrations in natural waters. Nature 324, 140–143.

Dahlgren, R.A., Walker, W.J., 1993. Aluminum release rates from selected Spodosol Bs horizons: effects of pH and solid-phase aluminum pools. Geochim. Cosmochim. Acta 57, 57–66.

DiChiaro, M.J., 1998. Mineralogy and cesium retention in a chronosequence of Hawaiian soils derived from volcanic debris. MS Thesis in Soil Science. The Pennsylvania State University, University Park, PA, 121 pp.

Dove, P.M., Crerar, D.A., 1990. Kinetics of quartz dissolution in electrolyte solutions using a hydrothermal mixed flow reactor. Geochim. Cosmochim. Acta 54, 955–969.

Fenchel, T., King, G.M., Blackburn, T.H., 1998. Bacterial Biogeochemistry: The Ecophysiology of Mineral Cycling. 2nd edn. Academic Press, San Diego.

Fiedler, S., 2000. In situ long-term measurement of redox potential in redoximorphic soils. In: Schuring, J. (Ed.), Redox: Fundamentals, Processes and Applications. Springer-Verlag, Berlin, pp. 81–94.

Furrer, G., Stumm, W. et al., 1986. The coordination chemistry of weathering: I. Dissolution kinetics of γ-Al_2O_3 and BeO. Geochim. Cosmochim. Acta 50, 1847–1860.

Furrer, G., Westall, J., Sollins, P., 1989. The study of soil chemistry through quasi-steady-state models: I. Mathematical definition of model. Geochim. Cosmochim. Acta 53, 595–601.

Furrer, G., Zysset, M., Schindler, P.W., 1993. Weathering kinetics of montmorillonite: investigations in batch and mixed-flow reactors. In: Manning, D.A.C. (Ed.), Geochemistry of Clay–Pore Fluid Interactions. Chapman & Hall, London, pp. 243–262.

Giambelluca, T.W., Nullet, M.A., Schroeder, T.A., 1986. Rainfall Atlas of Hawai'i. Department of Land and Natural Resources, State of Hawaii, Honolulu, HI. Report R76.

Gile, L.H., Grossman, R.B. et al., 1979. The Desert Project Soil Monograph. U.S. Government Printing Office, Washington, DC.

Harden, J.W., Taylor, E.M., Hill, C., Mark, R.K., McFadden, L.D., Reheis, M.C., Sowers, J.M., Wells, S.G., 1991. Rates of soil development from four chronosequences in the southern Great Basin. Quat. Res. 35, 383–399.

Hendricks, D.M., Chadwick, O.A., Gavenda, R.T., Kelly, E.F., Hsieh, J., 1995. Mineral transformation and evolution in a soil chronosequence in Hawaii. Agron. Abstr. Amer. Soc. Agron, p. 326. Madison, WI.

Hotchkiss, S., Vitousek, P.M., Chadwick, O.A., Price, J., 2000. Climate cycles, geomorphological change, and the interpretation of soil and ecosystem development. Ecosystems 3, 522–533.

Hsieh, J.C.C., Chadwick, O.A., Kelly, E.F., Savin, S.M., 1998. Oxygen isotopic composition of soil water: quantifying evaporation and transpiration. Geoderma 82, 269–293.

Huggett, R.J., 1998. Soil chronosequences, soil development and soil evolution: a critical review. Catena 32, 155–172.

Jackson, M.L., 1965. Clay transformations in soil genesis during the quaternary. Soil Sci 99, 15–22.

Jackson, M.L., Sherman, G.D., 1953. Chemical weathering of minerals in soils. Adv. Agron. 5, 219–318.

Jardine, P.M., Zelazny, L.W., 1996. Surface reactions of aqueous aluminum species. In: Sposito, G. (Ed.), The Environmental Chemistry of Aluminum. 2nd edn. CRC Press, Boca Raton, FL, pp. 221–270.

Johnson, D.L., Keller, E.A., Rockwell, T.K., 1990. Dynamic pedogenesis: new views on some key soil concepts, and a model for interpreting quaternary soils. Quat. Res. 33, 306–319.

Kelly, E.F., Chadwick, O.A., Hilinski, T., 1998. The effect of plants on mineral weathering. Biogeochemistry 42, 53–72.

Kennedy, M.J., Chadwick, O.A., Vitousek, P.M., Derry, L.A., Hendricks, D.M., 1998. Changing sources of base cations during ecosystem development, Hawaiian Islands. Geology 26, 1015–1018.

Langmuir, D., 1997. Aqueous Environmental Geochemistry. Prentice Hall, NJ.

Lasaga, A.C., 1998. Kinetic Theory in the Earth Sciences. Princeton Univ. Press, NJ.

Lerman, A., 1990. Transport and kinetics in surficial processes. In: Stumm, W. (Ed.), Aquatic Chemical Kinetics. Wiley, NY, pp. 505–534.

Lin, F.C., Clemency, C.V., 1981. The kinetics of dissolution of muscovites at 25°C and 1 atm CO_2 partial pressure. Geochim. Cosmochim. Acta 52, 143–165.

Lindberg, R.E., Runnells, D.D., 1984. Ground water redox reactions: an analysis of equilibrium state applied to Eh measurements and geochemical modeling. Science 225, 925–927.

Lindsay, W.L., 1979. Chemical Equilibria in Soils. Wiley, New York.

Lindsay, W.L., Walthall, P.M., 1996. The solubility of aluminum in soils. In: Sposito, G. (Ed.), The Environmental Chemistry of Aluminum. 2nd edn. CRC Press, Boca Raton, FL, pp. 333–362.

Lovley, D.R., 2000. Fe(III) and Mn(IV) reduction. In: Lovley, D.R. (Ed.), Environmental Microbe–Metal Interactions. ASM Press, Washington D.C., pp. 3–30.

Marshall, C.E., 1977. The Physical Chemistry and Mineralogy of Soils: II. Soils in Place. Wiley-Interscience, New York.

McBride, M.B., 1994. Environmental Chemistry of Soils. Oxford Univ. Press, New York.

McDonald, E.V., Pierson, F.B., Flerchinger, G.N., McFadden, L.D., 1996. Application of a soil water balance model to evaluate the influence of Holocene climate change on calcic soils, Mojave Desert, California. Geoderma 74, 167–192.

McFadden, L.D., 1988. Climatic influences on rates and processes of soil development in Quaternary deposits of southern California. Geol. Soc. Am. Spec. Pap. 216, 153–177.

McFadden, L.D., Knuepfer, P.L.K., 1990. Soil geomorphology: the linkage of pedology and surficial processes. Geomorphology 3, 197–205.

McFadden, L.D., Weldon, R.J., 1987. Rates and processes of soil development on Quaternary terraces in Cajon Pass, California. Geol. Soc. Am. Bull. 98, 280–293.
McKenzie, R.M., 1989. Manganese oxides and hydroxides. In: Dixon, J.B., Weed, S.B. (Eds.), Minerals in Soil Environments. 2nd edn. Soil Sci. Soc. Am., Madison, WI, pp. 439–465.
Morse, J.W., Casey, W.H., 1988. Ostwald processes and mineral paragenesis in sediments. Am. J. Sci. 288, 537–560.
Muhs, D.R., 1982. A soil chronosequence on Quaternary marine terraces, San Clemente Island, California. Geoderma 28, 257–283.
Muhs, D.R., 1984. Intrinsic thresholds in soil systems. Phys. Geogr. 5, 99–110.
Mulder, J., Stein, A., 1994. The solubility of aluminum in acidic forest soils: long-term changes due to acidic deposition. Geochim. Cosmochim. Acta 58, 85–94.
Nagy, K., 1995. Dissolution and precipitation kinetics of sheet silicates. In: White, A.F., Brantley, S.L. (Eds.), Chemical Weathering Rates of Silicate Minerals. Mineral. Soc. Am., Washington, DC, pp. 173–233.
Nahon, D.B., 1991. Introduction to the Petrology of Soils and Chemical Weathering. Wiley, New York.
Nightingale Jr., E.R., 1958. Poised oxidation–reduction systems. Anal. Chem. 30, 267–272.
Nordstrom, D.K., May, H.M., 1996. Aqueous equilibrium data for mononuclear aluminum species. In: Sposito, G. (Ed.), The Environmental Chemistry of Aluminum. 2nd edn. CRC Press, Boca Raton, FL, pp. 39–80.
Reid, D.A., Graham, R.C., Southard, R.J., Amrhein, C., 1993. Slickspot soil genesis in the Carrizo Plain, California. Soil Sci. Soc. Am. J. 57, 162–168.
Patrick Jr., W.H., Henderson, R.E., 1981. Reduction and reoxidation cycles of manganese and iron in flooded soil and water solution. Soil Sci. Soc. Am. J. 45, 855–859.
Patrick Jr., W.H., Jugsujinda, A., 1992. Sequential reduction and oxidation of inorganic nitrogen, manganese and iron in a flooded soil. Soil Sci. Soc. Am. J. 56, 1071–1073.
Reuss, J.O., Johnson, D.W., 1986. Acid deposition and the acidification of soils and waters. Springer-Verlag, New York.
Reuss, J.O., Walthall, P.M., Rosall, E.C., Hopper, R.W.E., 1990. Aluminum solubility, calcium–aluminum exchange and pH in acid forest soils. Soil Sci. Soc. Am. J. 54, 374–380.
Rimstidt, J.D., Barnes, H.L., 1980. The kinetics of silica–water reactions. Geochim. Cosmochim. Acta 44, 1683–1699.
Ritchie, G.S.P., 1995. Soluble aluminum in acidic soils: principles and practicalities. Plant Soil 171, 17–27.
Robarge, W.P., Johnson, D.W., 1992. Effects of acidic deposition on forested soils. Adv. Agron. 47, 1–83.
Scheidegger, A.M., Sparks, D.L., 1996. A critical assessment of sorption–desorption mechanisms at the soil mineral/water interface. Soil Sci. 161, 813–831.
Schnoor, J.L., 1990. Kinetics of chemical weathering: a comparison of laboratory and field weathering rates. In: Stumm, W. (Ed.), Aquatic Chemical Kinetics: Reaction Rates of Processes in Natural Waters. Wiley, NY.
Schumm, S.A., 1979. Geomorphic thresholds: the concept and its applications. Trans. Inst. Br. Geogr. 4, 485–515.
Schwertmann, U., Taylor, R.M., 1989. Iron oxides. In: Dixon, J.B., Weed, S.B. (Eds.), Minerals in Soil Environments. 2nd edn. Soil Sci. Soc. Am., Madison, WI, pp. 379–438.
Scott, R.M., 1963. Exchangeable bases of mature, well-drained soils in relation to rainfall in East Africa. J. Soil Sci. 13, 1–9.
Scott, M.J., Morgan, J.J., 1990. Energetics and conservative properties of redox systems. In: Melchior, D.C., Bassett, R.L. (Eds.), Chemical Modeling of Aqueous Systems II. Am. Chem. Soc. Symp., vol. 416, pp. 368–378.

Sexstone, A.J., Revsbech, N.P., Parkin, T.B., Tiedje, J.M., 1985. Direct measurement of oxygen profiles and denitrification rates in soil aggregates. Soil Sci. Soc. Am. J. 49, 645–651.

Soil Survey Staff, 1999. Soil Taxonomy. 2nd edn. USDA Agric. Handbook, vol. 436, U.S. Government Printing Office, Washington, DC.

Sparks, D.L., 1995. Environmental Soil Chemistry. Academic Press, San Diego.

Sposito, G., 1994. Chemical Equilibria and Kinetics in Soils. Oxford Univ. Press, NY.

Steefel, C.I., Van Capellen, P., 1990. A new approach to modeling water–rock interaction: the role of precursors, nucleation, and Ostwald ripening. Geochim. Cosmochim. Acta 54, 2657–2677.

Stewart, B.W., Capo, R.C., Chadwick, O.A., 2001. Effect of rainfall on weathering rate, base cation provenance, and Sr isotope composition of Hawaiian soils. Geochim. Cosmochim. Acta (in press).

Stumm, W., 1992. Chemistry of the Solid–Water Interface. Wiley, NY.

Stumm, W., Morgan, J.J., 1996. Aquatic Chemistry: Chemical Equilibria and Rates in Natural Waters. 3rd edn. Wiley, NY.

Stumm, W., Wollast, R., 1990. Coordination chemistry of weathering, kinetics on the surface-controlled dissolution of oxide minerals. Rev. Geophys. 28, 53–69.

Suarez, D.L., Goldberg, S., 1994. Modeling soil solution, mineral formation and weathering. In: Bryant, R.B., Arnold, R.W. (Eds.), Quantitative Modeling of Soil Forming Processes. SSSA Spec. Publ., vol. 39, Soil Sci. Soc. Am., Madison, WI.

Sverdrup, H., Warfvinge, P., 1995. Estimating field weathering rates using laboratory kinetics. In: White, A.F., Brantley, S.L. (Eds.), Chemical Weathering Rates of Silicate Minerals. Rev. Miner., vol. 31, Min. Soc. Am, Washington D.C., pp. 485–542.

Swodoba-Colberg, N.G., Drever, J.D., 1993. Mineral dissolution rates in plot-scale field and laboratory experiments. Chem. Geol. 105, 51–69.

Teichert, A., Bottcher, J., Duijnisveld, W.H.M., 2000. Redox measurements as a qualitative indicator of spatial and temporal variability of redox state in a sandy forest soil. In: Schuring, J. (Ed.), Redox: Fundamentals. Processes and Applications. Springer-Verlag, Berlin, pp. 95–110.

Thomas, G.W., Hargrove, W.L. et al., 1984. The chemistry of soil acidity. In: Adams, F. (Ed.), Soil Acidity and Liming. American Society of Agronomy, Madison, WI.

Torrent, J., Nettleton, W.D., 1978. Feedback processes in soil genesis. Geoderma 20, 281–287.

Ugolini, F.C., Dahlgren, R., 1987. The mechanism of podzolization as revealed through soil solution studies. In: Righi, D., Chauvel, A. (Eds.), Podzols and Podzolization. INRA, Paris, pp. 195–203.

Ugolini, F.C., Mann, D.H., 1979. Biopedological origin of peatlands in Southeast Alaska. Nature 281, 366–368.

Ugolini, F.C., Sletten, R.S., 1991. The role of proton donors in pedogenesis as revealed by soil solution studies. Soil Sci. 151, 59–75.

Ugolini, F.C., Dahlgren, R., Shoji, S., Ito, T., 1988. An example of andolization and podzolization as revealed by soil solution studies, southern Hakkoda, northeastern Japan. Soil Sci. 145, 111–125.

van Breemen, N., 1995. How Sphagnum bogs down other plants. TREE 10, 270–275.

van Breemen, N., Mulder, J., Driscoll, C.T., 1983. Acidification and alkalization of soils. Plant Soil 75, 283–308.

van Breemen, N., Driscoll, C.T., Mulder, J., 1984. Acidic deposition and internal proton sources in acidification of soils and waters. Nature 307, 599–604.

Vance, G.F., Stevenson, F.J., Sikora, F.J., 1996. Environmental chemistry of aluminum–organic complexes. In: Sposito, G. (Ed.), The Environmental Chemistry of Aluminum. 2nd edn. CRC Press, Boca Raton, FL, pp. 169–220.

van Grinsven, J.J.M., van Riemsdijk, W.H., 1992. Evaluation of batch and column techniques to measure weathering rates in soils. Geoderma 52, 41–57.

Velbel, M.A., 1993. Constancy of silicate-mineral-weathering ratios between natural and experimental weathering: implications for hydrologic control of differences in absolute rate. Chem. Geol. 105, 89–99.

Vitousek, P.M., Chadwick, O.A., Crews, T., Fowns, J., Herbert, D., Hendricks, D.M., 1997. Soil and ecosystem development across the Hawaiian Islands. GSA Today 7 (9), 1–8.

Vitousek, P.M., Kennedy, M.J., Derry, L.A., Chadwick, O.A., 1999. Weathering versus atmospheric sources of strontium in ecosystems on young volcanic soils. Oecologia 121, 255–259.

von der Kammer, F., Thoming, J., Forstner, U., 2000. Redox buffer capacity concept as a tool for the assessment of long-term effects in natural attenuation/intrinsic remediation. In: Schuring, J. (Ed.), Redox: Fundamentals Processes and Applications. Springer-Verlag, Berlin, pp. 189–202.

Wells, S.G., McFadden, L.D., Dohrenwend, J.C. et al., 1987. Influences of late Quaternary climatic changes on geomorphic and pedogenic processes on a desert piedmont, eastern Mojave Desert, California. Quat. Res. 27, 130–146.

White, A.F., Blum, A.E., Schulz, M.S., Bullen, T.D., Harden, J.W., Peterson, M.L., 1996. Chemical weathering rates of a soil chronosequence on granitic alluvium: I. Quantification of mineralogical and surface area changes and calculation of primary silicate reaction rates. Geochim. Cosmochim. Acta 60, 2533–2550.

Wieland, E., Stumm, W., 1992. Dissolution kinetics of kaolinite in acidic aqueous solutions at 25°C. Geochim. Cosmochim. Acta 56, 3339–3355.

Yaalon, D.H., 1971. Soil-forming processes in space and time. In: Yaalon, D.H. (Ed.), Paleopedolology—Origin, Nature and Dating of Paleosols. Israel Univ. Press, Jerusalem, pp. 29–39.

Yeh, G.T., Iskra, G.A., Szecsody, J.E., Zachara, J.M., Streile, G.P., 1995. KEMOD: A mixed chemical kinetic and equilibrium model of aqueous and solid phase geochemical reactions. Tech. Report PNL 10380, Battelle.